



# Eigenvalue curve veering in stressed structures: An experimental study

Jonathan Luke du Bois<sup>a,\*</sup>, Sondipon Adhikari<sup>b</sup>, Nick A.J. Lieven<sup>a</sup>

<sup>a</sup>*Department of Aerospace Engineering, University of Bristol, Queens Building, University Walk, Bristol BS8 1TR, UK*

<sup>b</sup>*School of Engineering, Swansea University, Singleton Park, Swansea SA2 8PP, UK*

Received 20 November 2007; received in revised form 17 November 2008; accepted 3 December 2008

Handling Editor: C.L. Morfey

Available online 18 January 2009

---

## Abstract

There have been extensive research works on the veering phenomenon in dynamic systems. As eigenvalues change under parametric variation, converging loci are commonly seen to veer away suddenly in a small region of the graph such that the modes swap trajectories. All of the modal properties are swapped in the process, leading to some curious behaviour in the transition zone. Theoretical studies of this behaviour have been reported for half a century but despite this heritage, explicit references to experimental results are scarce. In this paper detailed experimental and numerical investigations on veering are reported. The parameter varied is the internal pre-load of a redundant frame. An FE model is presented and stress stiffening approximations are employed to obtain a tangent stiffness for a nonlinear static solution, which is then used in a linear dynamic analysis. Experimental results are given and the behaviour is found to correspond well with the analytical results. In particular the mode shape variation is found to be consistent, and the implications of this finding with regard to modal correlation and model validation are noted. Analyses of the mode shapes in terms of eigenvector rotations are presented and are found to form a valuable tool for the interpretation of experimental results.

© 2008 Elsevier Ltd. All rights reserved.

---

## 1. Introduction

The eigenvalue loci of a dynamic system subject to parametric variation are often observed to follow intersecting trajectories. Interaction of the modes in these regions may lead to the loci veering from their nominal trajectories. Commonly, they are seen to veer abruptly away from each other so that after veering each locus continues on the path previously followed by the other. The modes effectively swap properties in this region; as well as the rapid change in eigenvalue sensitivities, the mode shapes undergo violent transformations in the transition. Some illuminating illustrations can be found in Refs. [1–3].

Early observations of the behaviour in structural dynamics were highlighted by Claassen and Thorne [4]. Leissa [5] cited further examples to draw attention to the possibility of fallacious artefacts in numerical models, and demonstrated that veering could be artificially induced through inadequate approximations and

---

\*Corresponding author. Tel.: +44 117 331 7367.

E-mail address: [jon.dubois@bristol.ac.uk](mailto:jon.dubois@bristol.ac.uk) (J.L. du Bois).

discretisations. Later, Kuttler and Sigillito [6] used rigorous error bounds to confirm the existence of curve veering in accurate mathematical models and Perkins and Mote [7] adapted Schajer's work [8] to present an exact mathematical solution exhibiting the behaviour. More recent works have found application for the theory, for example in the prediction of flutter in rotating blade assemblies [9].

Despite widespread acceptance of veering theory, supporting experimental data are scarce, if not absent, in the literature. Such evidence is inferred in many cases: for example, the orthotropic plate experiments detailed by McIntyre and Woodhouse [10] rely on the manifestation of veering, and there is a wealth of data relating to rotor tuning in turbomachinery where mistuned blades and coupling between shaft and blade vibration modes lead to the related phenomena of localisation [11] and veering [12]. These do not provide categorical substantiation, however, and this paper is intended to provide an unambiguous experimental demonstration of the effect.

Knowledge of the interactions of proximate modes provides valuable insight in a wide range of practical activities. Any analyses relying on assumptions regarding the coupling between modes, or a lack thereof, will be influenced by the concepts contained herein. Such methodologies include modal parameter extraction, system identification and updating, uncertainty analysis, modal control, localisation, statistical energy analysis, high and mid-frequency vibration and modal analysis itself.

## 2. An overview of mode veering

Pierre [13] explains how localisation and veering are related to two “couplings”: the physical coupling between component structures, and the modal coupling seen between mode shapes through parameter perturbations. He asserts that localisation and veering occur when this modal coupling is of the same order or greater than the physical coupling.

Perkins and Mote [7] use perturbation theory to derive “coupling factors” to quantify the eigenfunction coupling. Their work demonstrates that modes in self-adjoint eigenproblems will always veer away from each other as described in this paper, except in the limiting case of zero modal coupling where they may cross. Small coupling factors lead to rapid curve veering, but large coupling factors produce less remarkable parametric variation in the eigenstructure. Liu [14] suggests defining a critical value for the derivative of the eigenvectors or for the second derivative of the eigenvalues, above which the modes would be deemed to be veering.

Many authors have noted that a symmetric mode's frequency locus will always cross that of an antisymmetric mode while two symmetric or two antisymmetric modes will generally veer [1–3,7,15]. As such, the introduction of small asymmetries to a symmetric system will result in instances of rapid veering. This is the case for the structure examined in this paper.

Both Woodhouse [16] and Adhikari [17,18] cite examples where veering is influenced and sometimes even suppressed by the effects of damping. It is noted, however, that these cases depend on a non-trivial level of unevenly distributed damping throughout the structure. The structure considered here has very low, approximately uniform damping, permitting the use of real approximations for the experimental mode shape identification.

Balmès [19] analysed the eigenvector transformations of a three degree of freedom (dof) lumped-mass system in terms of the vector rotations within a fixed subspace. His system used the identity matrix as a mass matrix and thus produced orthogonal eigenvectors in the physical coordinate system. These were seen to rotate smoothly as the two frequency loci veered, asymptotically revolving through 90° to facilitate the swapping of the mode shapes. In this paper the eigenvector rotations will be used to provide a quantitative measure of the mode shape transformations. The analysis will take advantage of the fact that the modal assurance criterion (MAC), as a squared inner product of two normalised eigenvectors, corresponds to the squared cosine of the angle between the vectors:

$$\text{MAC}_{jk} = \cos^2 \alpha_{jk} = (\psi_j^T \psi_k)^2 / (\psi_j^T \psi_j)(\psi_k^T \psi_k) \quad (1)$$

## 3. Experimental setup

The structure used to demonstrate the behaviour is a redundant truss, pictured in Fig. 1. The cross-braced rectangle creates a static redundancy, such that shortening one of the members distributes a load throughout

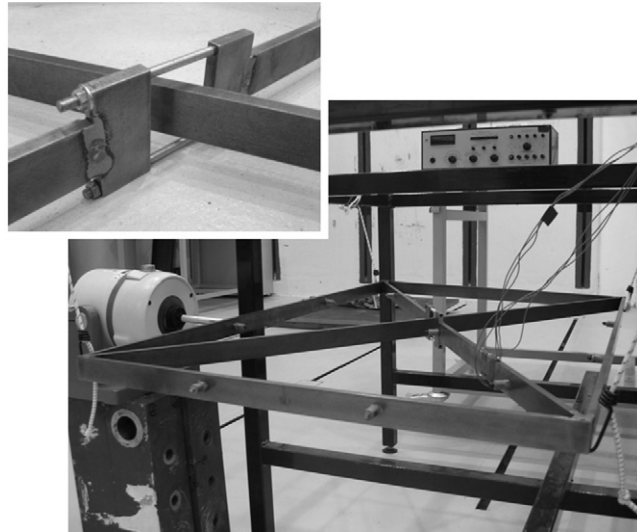


Fig. 1. Experimental setup, with a close up of the tensioning mechanism inset.

the truss. Loading the structure induces the well-known nonlinear effect of stress stiffening, whereby the transverse stiffness of the beams is influenced by the applied axial loads. This modulation of the structural stiffness is used to provide the parametric variation for the current experiment.

The tensioning is accomplished using two bolts, mounted in flanges in one of the diagonal members and passing either side of the other cross-beam so that there is no contact. Strain gauges are mounted on top and bottom of the adjustable member to measure the load and ensure that no bending moment is induced. The  $8 \times 30$  mm beam cross-section creates good separation between the in-plane and out-of-plane vibration modes and the corner joints are welded with all of the beam centrelines in one plane to avoid coupling between the two sets of modes. The outside dimensions of the rectangle are  $1000 \times 600$  mm.

The framework is suspended by bungee cords and 12 accelerometers are distributed with two positioned evenly along the length of each member. Two additional accelerometers are fitted either side of the bolt flanges in the tensioning member. A shaker is used to supply broadband excitation and five runs are used at each load to compute averaged frequency response functions (FRFs) in the 0–256 Hz range with 1024 spectral lines. The modal parameters are identified using the time domain least squares complex exponential (LSCE) and least squares frequency domain (LSFD) methods [20,21].

#### 4. Finite element (FE) model

The approach adopted for the FE model is to first use a nonlinear static analysis to determine the tangent stiffness for a given load case. Then, assuming small dynamic loads and displacements, the tangent stiffness is used to obtain a linear dynamic solution. The nonlinear technique is described in textbooks such as Cook [22].

The model uses six two-dimensional Euler–Bernoulli beam elements to represent each member of the frame. The tensioning mechanism is represented by a further three elements, two for the flanged beam sections and one for the bolts. The static loading is modelled by first removing the axial coupling between the bolts and the flange at one end of the mechanism and fully constraining all the dofs at the free end of the flange. An axial load is then applied to the free end of the bolts while constraining the transverse and rotational motion. Once the static solution is obtained, the dofs at the two free ends can be coupled and the constraints removed to obtain the free dynamic response. The effects of stress stiffening are included in the dynamic analysis using methods set out by Jennings [23] in conjunction with Newton–Raphson iterations.

Following common practice for nonlinear buckling analyses [24], a small perturbation is introduced to the straight members of the FE model to encourage instability. This symmetric alteration has negligible effects away from the buckling load but is described here for completeness. The perturbation takes the form of a

sinusoidal transverse curvature in the long outside members of the frame. An amplitude of 0.185% of the member length is chosen by inspection to reconcile the analytic and experimental buckling behaviour.

## 5. Results

The structure was tensioned in approximately 273 N increments (corresponding to  $5 \mu\epsilon$ ), tightening the bolts incrementally until it was deemed to have buckled at 6800 N. The eigenfrequencies are presented in Fig. 2(a), and good correlation is seen between these and the eigenfrequencies from the FE model, plotted in Fig. 2(b) using 300 N load steps.

The loci appear to cross in several places. The point where modes 5 and 6 meet at around 3500 N will be examined in detail. The mode shapes produced by the FE model for modes 5 and 6 are found to have “even” and “odd” rotational symmetry, respectively. Following the discussion in Section 2 they are therefore expected to cross rather than veer, and this is seen to be the case in Fig. 3(a). In a practical structure, however, perfect symmetry cannot be achieved. The greatest source of uncertainty in this model is at the welded joints. Accordingly, a weak weld in one of the joints is introduced to the FE model to break the symmetry. The weakness is simulated by including a short beam element of reduced width at one end of the non-adjustable diagonal member. The beam length is 21 mm and the width is reduced in 10% increments. Fig. 3(b) shows the results for the 30% case, where the modified FE model is seen to exhibit veering closely matching the behaviour of the physical structure plotted in Fig. 3(c).

The experiment was conducted on two occasions, separated by a period of months, to ensure repeatability. Both sets of results exhibit the same trends, and the MAC provides an unambiguous correlation between the two modes from one load step to the next: the diagonal elements of the MAC matrix never drop below 0.79, while the off-diagonal terms never exceed 0.41. To further corroborate this result, the well-established FE modes are analysed using the MAC at the same intervals and produce comparable values: the lowest diagonal element is 0.77 and the highest off-diagonal is 0.34.

The mean damping ratios for the two modes were found to be  $1.14 \times 10^{-3}$  and  $1.20 \times 10^{-3}$ , and showed no significant variation throughout the loading regime. This justifies the use of real approximations to the mode shapes. The mode shape variation throughout veering is shown in Fig. 4, where the analytic and experimental results are seen to correspond well. After veering each mode takes on the form of the other through a continuous transformation. To better quantify the mode shape transformations, the fifth eigenvector at 2000 N is chosen as a reference and the orientation of the two eigenvectors throughout the veering region is calculated relative to this datum. The analytic results are once again in good agreement with the FE data, witnessed in Fig. 5. Similarly to Balmès’ example [19], the vectors are almost orthogonal and rotate smoothly

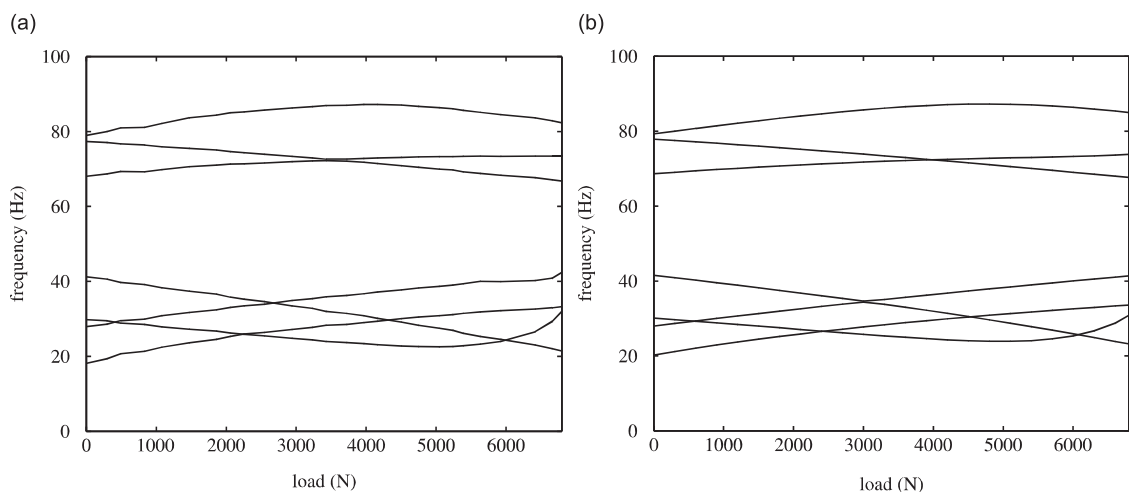


Fig. 2. The first seven eigenfrequency loci plotted with varying load: (a) experimental data; (b) FE model.

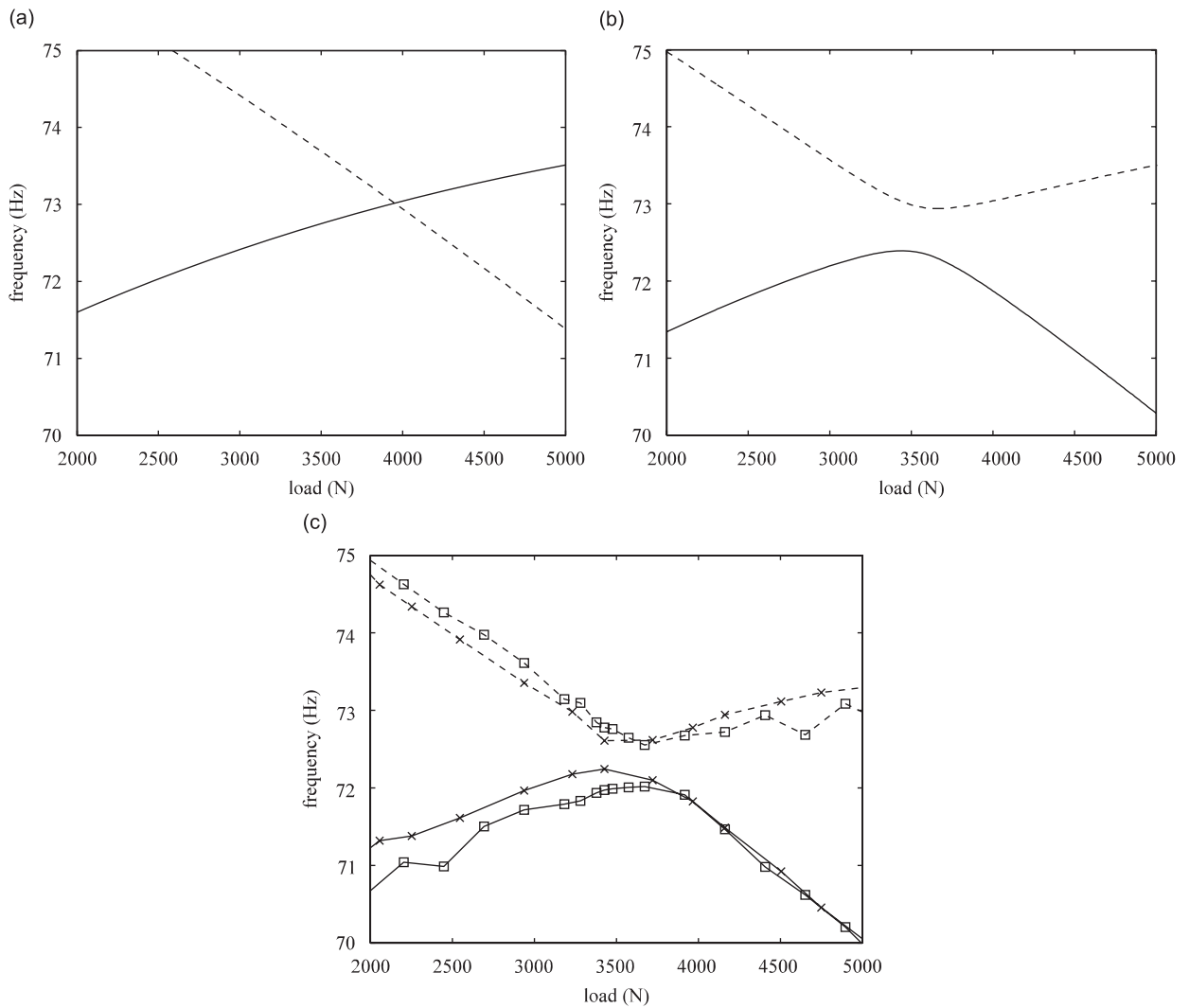


Fig. 3. Close examination of the interaction between the fifth (—) and sixth (---) modes. FE models use adaptive loadsteps, down to 2.25 N at maximum curvature. (a) Symmetric FE model exhibits crossing. (b) Asymmetric FE model exhibits veering. (c) Both sets of experimental data (× and □) match the trends of the asymmetric model.

through nearly  $90^\circ$ . In this case the vector orthogonality in the physical coordinate system is attributed to the even mass distribution in the structure.

These observations have several ramifications. Saliiently, the rapid eigenvector transformations and changing eigenvalue sensitivities will pose difficulties for modal correlation and sensitivity-based updating schemes, particularly where a symmetric model has erroneously been assumed. More generally, the sensitive variation of modal properties will have implications in any study with unmodelled complexities or uncertain parameters and such analyses may be aided by careful interpretation of the vector rotations as presented here.

To exemplify the benefit of a through understanding of the mode shape transformations, their influence on the response functions is examined below. For any proximate modes the total response within the frequency band is independent of the orientation of the vectors and depends only on the subspace they define [19]. In general this means that veering has limited impact on the response. Igusa [25] discusses exceptions to this rule where the response magnitude can be highly sensitive to modal interactions. Such an example exists for the current structure using response and excitation points on opposite sides of the frame along its longitudinal axis. The analytical FRFs presented in Fig. 6 show that in the symmetric FE model the response dips as the

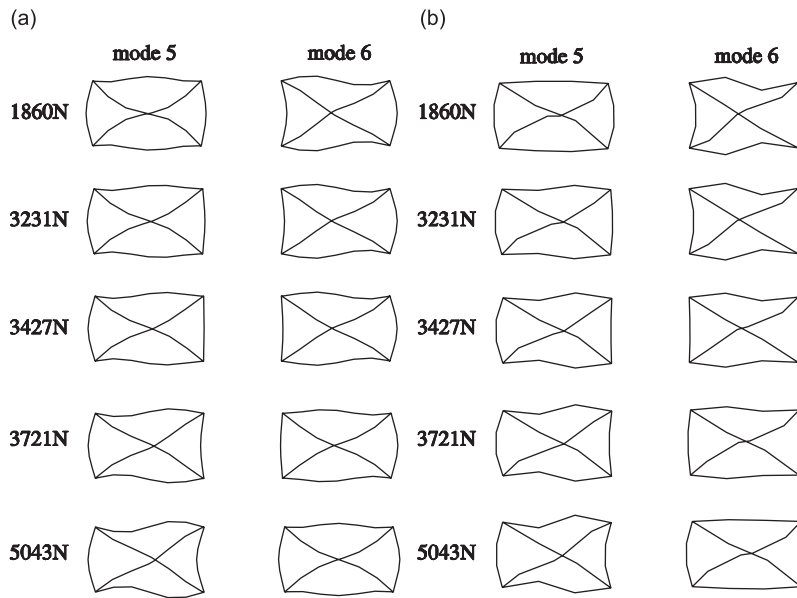


Fig. 4. Mode shape variations as modes 5 and 6 veer. The eigenvectors transform smoothly so that after veering the two modes have swapped, with one mode taking on the inverted form of the other prior to veering: (a) FE model; (b) experimental results.

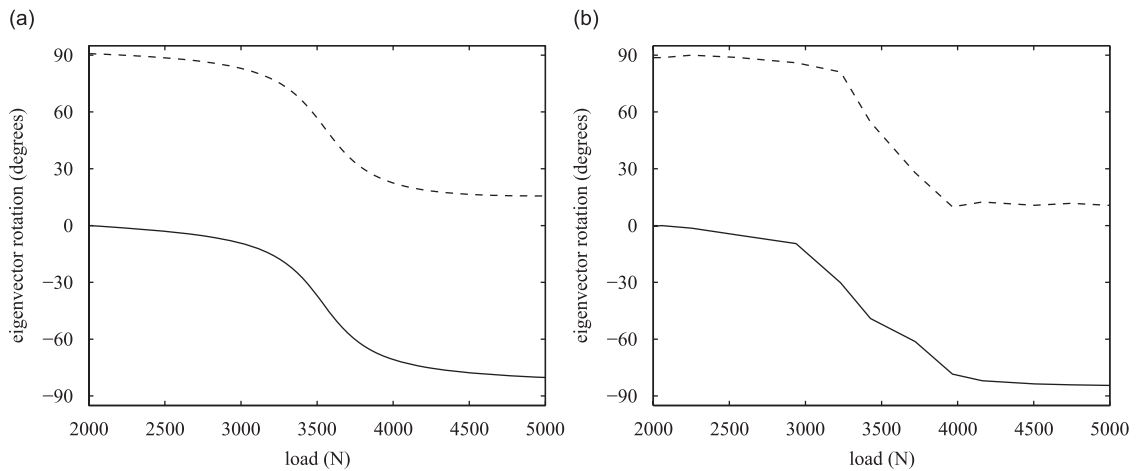


Fig. 5. Eigenvector rotations of the fifth (–) and sixth (– –) modes: (a) FE model; (b) experimental data.

modes interact. The modal superposition produces a cancellation of the two modes at this point. Intuitively, veering would lessen this effect as the modes are never coincident. In contrast, however, the results from the asymmetric model show that a dip remains present in each of the resonant ridgelines, and in fact spans a greater load range than in the symmetric model. This is mirrored in the experimental data. The modified behaviour is no longer caused by modal superposition but is instead caused by the individual mode shape transformations. Increasing the asymmetry and hence the modal coupling slows down the veering process and the resultant effect is similar to that produced by increased damping. Without an appreciation for the effects of modal interactions such behaviour would be difficult to rationalise and consequently difficult to suppress or exploit.

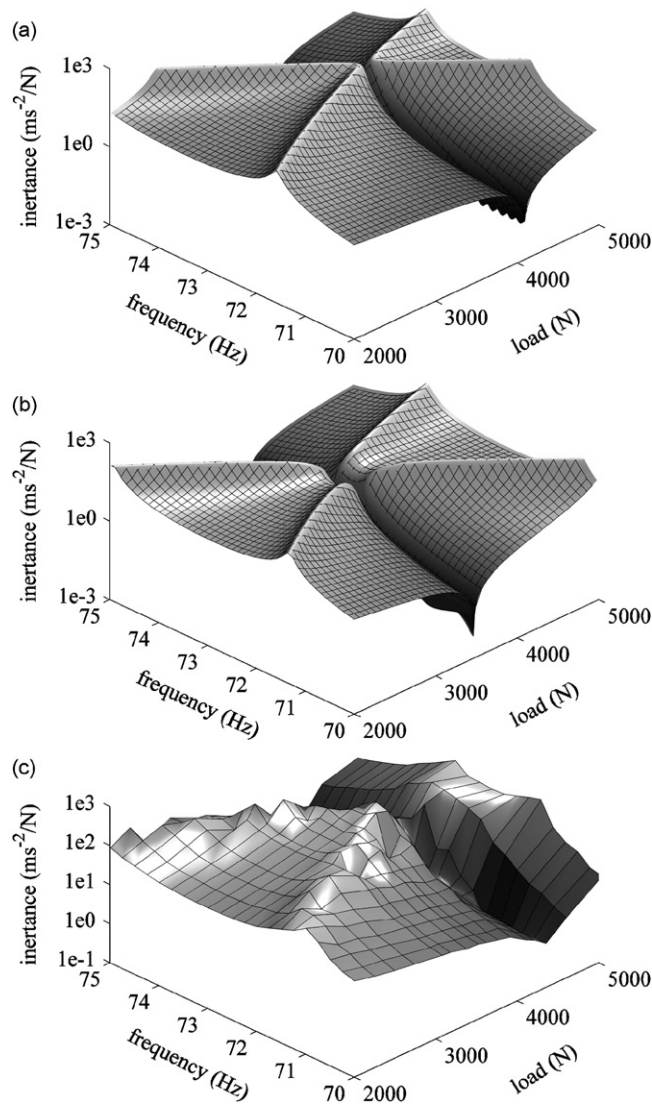


Fig. 6. FRFs in the veering region. Analytical model uses uniform modal damping ratios of  $1.2 \times 10^{-3}$ : (a) Symmetric FE model; (b) asymmetric FE model; (c) experimental data.

## 6. Conclusion

A clear experimental demonstration of curve veering has been given and the results shown to correspond well with those predicted by finite element modelling. In particular the counterintuitive variations of the mode shapes in these regions have been confirmed. The investigation has highlighted the impact of veering on model updating and modal correlation algorithms, as well as any discipline concerned with the analysis of closely spaced modes. The examination of the mode shape transformations in terms of eigenvector rotations is found to be a valuable tool in quantifying the behaviour and this is expected to find application in a wide range of parametric modal analyses.

## References

- [1] M. Petyt, C.C. Fleischer, Free vibration of a curved beam, *Journal of Sound and Vibration* 18 (1) (1971) 17–30.
- [2] P.S. Nair, S. Durvasula, On quasi-degeneracies in plate vibration problems, *International Journal of Mechanical Sciences* 15 (1973) 975–986.

- [3] M.S. Triantafyllou, The dynamics of taut inclined cables, *Quarterly Journal of Mechanics and applied Mathematics* 37 (3) (1984) 421–440.
- [4] R.W. Claassen, C.J. Thorne, Vibrations of a rectangular cantilever plate, *Journal of the Aerospace Sciences* 29 (11) (1962) 1300–1305.
- [5] A.W. Leissa, On a curve veering aberration, *Journal of Applied Mathematics and Physics* 25 (1974) 99–111.
- [6] J.R. Kuttler, V.G. Sigillito, On curve veering, *Journal of Sound and Vibration* 75 (4) (1981) 585–588.
- [7] N.C. Perkins, C.D. Mote Jr, Comments on curve veering in eigenvalue problems, *Journal of Sound and Vibration* 106 (3) (1986) 451–463.
- [8] G.S. Schajer, The vibration of a rotating circular string relative to a fixed end restraint, *Journal of Sound and Vibration* 92 (1) (1984) 11–19.
- [9] D. Afolabi, O. Mehmed, On curve veering and flutter of rotating blades, *Journal of Engineering for Gas Turbines and Power* 116 (1994) 702–708.
- [10] M.E. McIntyre, J. Woodhouse, On measuring the elastic and damping constants of orthotropic sheet materials, *Acta Metallurgica* 36 (6) (1988) 1397–1416.
- [11] Y.-J. Chiu, S.-C. Huang, The influence on coupling vibration of a rotor system due to a mistuned blade length, *International Journal of Mechanical Sciences* 49 (2007) 522–532.
- [12] Ö. Turhan, G. Bulut, Linear coupled shaft-torsional and blade-bending vibrations in multi-stage rotor-blade systems, *Journal of Sound and Vibration* 296 (2006) 292–318.
- [13] C. Pierre, Mode localization and eigenvalue loci veering phenomena in disordered structures, *Journal of Sound and Vibration* 126 (3) (1988) 485–502.
- [14] X.L. Liu, Behaviour of derivatives of eigenvalues and eigenvectors in curve veering and mode localisation and their relation to close eigenvalues, *Journal of Sound and Vibration* 256 (3) (2002) 551–564.
- [15] J.J. Webster, Free vibrations of rectangular curved panels, *International Journal of Mechanical Science* 10 (1968) 571–582.
- [16] J. Woodhouse, On the synthesis of guitar plucks, *Acta Acustica united with Acustica* 90 (2004) 928–944.
- [17] S. Adhikari, Rates of change of eigenvalues and eigenvectors in damped dynamic system, *AIAA Journal* 39 (11) (1999) 1452–1457.
- [18] S. Adhikari, Derivative of eigensolutions of non-viscously damped linear systems, *AIAA Journal* 40 (10) (2002) 2061–2069.
- [19] E. Balmès, High modal density, curve veering, localization: a different perspective on the structural response, *Journal of Sound and Vibration* 161 (2) (1993) 358–363.
- [20] H. Vold, J. Kundrat, G.T. Rocklin, R. Russel, Multi-input modal estimation algorithm for minicomputers, SAE Transactions.
- [21] B. Peeters, G. Lowet, H.V. der Auweraer, J. Leuridan, A new procedure for modal parameter estimation, *Sound and Vibration* (2004) 24–28.
- [22] R.D. Cook, *Concepts and Applications of Finite Element Analysis*, Wiley, New York, 1974.
- [23] A. Jennings, Frame analysis including change of geometry, *Proceedings of the ASCE, Journal of the Structural Division* 94 (1968) 627–644.
- [24] O.C. Zienkiewicz, *The Finite Element Method*, third ed., McGraw-Hill Book Company, London, 1977.
- [25] T. Igusa, Critical configurations of systems subjected to wide-band input, *Journal of Sound and Vibration* 168 (3) (1993) 525–541.